JOURNAL OF MATERIALS SCIENCE 10 (1975) 737-746

The formation of hydrogen-filled cavities in MgO crystals annealed in reducing atmospheres

A. BRIGGS
Materials Development Division, AERE, Harwell, Didcot, Oxon, UK

Defects causing cloudiness in some MgO crystals annealed in reducing atmospheres are shown to be lenticular cavities up to 200 μm diameter, containing hydrogen gas under high pressure. A close connection between the formation of cavities and the hydroxyl impurity content of the crystals is established, and a mechanism for their formation proposed, involving the reaction of oxygen vacancies and electrons, created at the surface, with V_{OH} centres in the interiors of the crystals. On the basis of these results and work by Amelinckx *et al.* and Barr *et al.* a general principle is postulated, in which a special gaseous environment, by reacting with a crystal surface, causes a second reaction within the crystal which converts an anion impurity into a permanent gas and produces gas-filled cavities. This principle may be applicable to many ionic crystal/reducing gas systems.

1. Introduction

A close relationship between cavities and hydroxyl impurity distribution in as-grown MgO crystals produced by solidification from the melt was demonstrated by Briggs [1]. The cavities were octahedral or cubo-octahedral, with sizes in the range 10^3 to 10^4 Å, and contained hydrogen gas under high pressure. They imparted a cloudy appearance to the central regions of the crystals by scattering light. For the purpose of irradiation damage experiments described by Henderson *et al.* [2], specimens cleaved from optically clear regions of such crystals were annealed in hydrogen to reduce ferric to ferrous iron. After this treatment, many of the specimens had cloudy central regions which gave them an appearance reminiscent of the cloudy as-grown crystals described by Briggs [1]. The similarity in appearance to the as-grown crystals suggested that the light-scattering defects in hydrogen-annealed crystals might also be cavities, and this paper describes the investigation of their nature and the mechanism of their formation.

2. Experimental

After heating for several hours at 1250° C, in an atmosphere of flowing hydrogen, the central regions of some previously clear MgO crystals appeared cloudy to the unaided eye. Other crystals remained quite clear. Ultramicroscopy showed the cloudiness to be due to light-scattering by two types of defect.

(a) Thin lenticular defects, up to ~ 200 μm diameter, lying close to {100} planes. They were often bounded, in these planes, by straight edges parallel to ⟨110⟩ directions, as shown in Fig. 1a, but more often had irregular perimeters. Seen perpendicular to the view shown in Fig. 1a they appeared as thin ellipses, as in Fig. 1b. They occurred both on sub-grain boundaries and in sub-grain interiors.

(b) Much smaller defects, resolvable by ultramicroscopy only as points of light, but revealed by transmission electron microscopy as polyhedral cavities. They were much more numerous than the bigger defects, but had a similar geographical distribution.

Precision density measurements, using a density gradient column, showed that specimens containing the defects were less dense than untreated specimens, and this was so whether the defects were predominantly of the larger or smaller variety. The density, shown in Table I, indicated that defects of both types were cavities.

Heating for several hours in either deuterium or carbon monoxide also produced cavities in specimens from the same crystal. When specimens annealed in hydrogen, deuterium or carbon

© *1975 Chapman and Hall Ltd.*

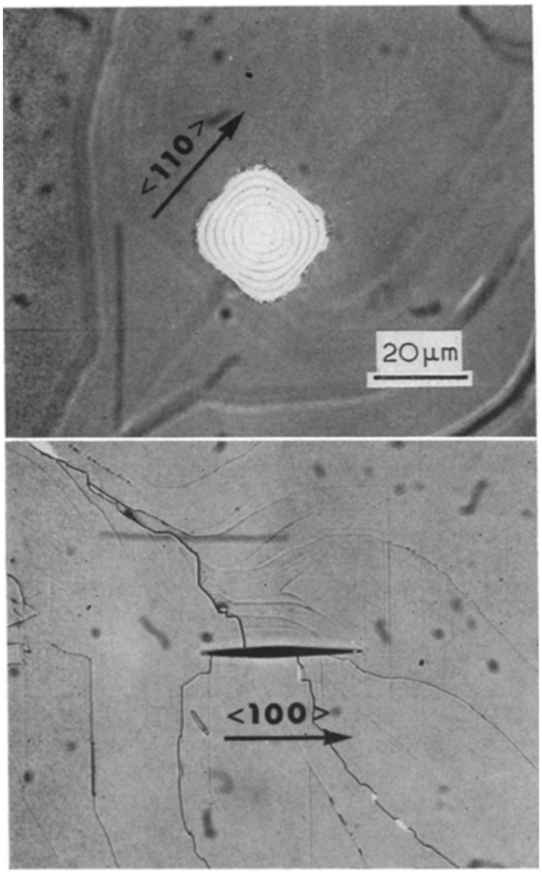

Figure 1 (a) A lenticular cavity seen in plan view, in monochromatic, reflected light. (b) A similar cavity seen in cross-section.

TABLE I Precision density measurements

Specimen treatment	Density (g cm^{-3})	Comments
Untreated	3.584 54 ± 0.000 10	Average of three specimens
Annealed in H_2 for 20 h at 1250°C	3.583 93 ± 0.000 10	Mainly larger defects
	3.583 57 ± 0.000 10	Mainly smaller defects

monoxide were dissolved slowly in hot acid they released bubbles of gas at the sites of cavities, and when such specimens were crushed and the gas released was analysed by mass spectrometer, hydrogen only was detected. The possibility that hydrogen from the annealing atmospheres diffused into the crystals can be discounted for the following reasons: hydrogen would not diffuse in preference to deuterium because the "mass effect" on the diffusion of hydrogen isotopes is so small [3] yet no deuterium was detected in the cavities in crystals annealed in deuterium. Analysis of the carbon monoxide by mass-spectrometer showed that it contained no detectable hydrogen impurity. Since hydrogen-filled cavities were produced by annealing crystals in hydrogen, deuterium or carbon monoxide, and the hydrogen could not have diffused in from the surface, it is clear that the source of the gas in the cavities must be hydrogen impurity within the crystals. Hydrogen was present in the cavities whether the specimens were cooled slowly or quenched from the annealing temperature, which indicates that the gas accumulated as the cavities formed. The fact that a variety of reducing gases produced similar effects suggests that a key factor in the production of hydrogen-filled cavities may be a reduction process occurring at the crystal surfaces. Annealing in oxygen or argon produced no such effects.

3. The pressure of gas in the cavities

The volumes of lenticular cavities were calculated from their thicknesses, which were determined by interference microscopy. When viewed perpendicular to their faces in monochromatic, reflected light, the cavities exhibited interference fringes, as seen in Fig. 1a. It may be shown that, for a cavity of varying thickness, d (Å) the first fringe appears where $d = 0$, and the nth fringe where $d = [(n - 1)/2]\lambda$, where λ is the wave-

TABLE II Gas pressure in cavities in H_2-annealed crystals

Cavity number	Cavity volume (cm^3)	Bubble volume (cm^3)	Cavity pressure (atm)
1	8.7×10^{-10}	1.3×10^{-7}	149
2	8.7×10^{-10}	4.0×10^{-7}	459
3	6.1×10^{-10}	1.9×10^{-7}	312
4	8.7×10^{-10}	2.7×10^{-7}	310
5	7.0×10^{-9}	1.27×10^{-6}	182
6	8.7×10^{-10}	5.7×10^{-7}	655
7	1.8×10^{-9}	2.5×10^{-7}	143*
8	2.5×10^{-10}	1.1×10^{-7}	435
9	3.1×10^{-10}	2.8×10^{-7}	900
10	4.5×10^{-10}	3.2×10^{-7}	710
11	4.7×10^{-11}	7.8×10^{-8}	600
12	3.0×10^{-10}	4.1×10^{-8}	138*
13	5.2×10^{-11}	7.5×10^{-9}	144

*Probably more accurate than the rest because the cavity thicknesses were determined from Newton fringes.

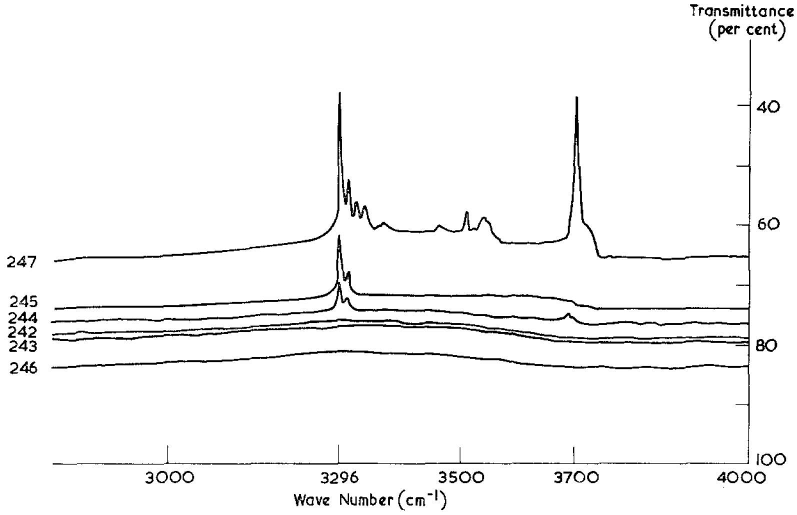

Figure 2 Infra-red spectra from crystals of MgO that do produce cavities (244, 245 and 247) and that do not produce cavities (242, 243 and 246). The spectrum for 247 has been moved 20% up the transmittance axis for the sake of clarity.

length of the light used. In this case the light was green, with $\lambda = 5500$ Å. The thickness of the cavity in Fig. 1a at its mid-point is, therefore, 1.93 μm. The bubble release and measurement technique described in [1] was used to obtain the volume of gas in the cavities, and this volume was related to the cavity volume to determine the pressure of the gas. Gas pressures in thirteen cavities are given in Table II.

4. Relationship between hydroxyl content and ability to form cavities on annealing in hydrogen

Specimens selected from three crystals (two

TABLE III OH^- content of crystals

Specimen number	Peak wave number (cm^{-1})	Number of OH^- ions per cm^3 before annealing in hydrogen	after annealing in hydrogen
242*	3296	$< 10^{14}$	$< 10^{14}$
	3310	$< 10^{14}$	$< 10^{14}$
243*	3296	$< 10^{14}$	4×10^{14}
	3310	$< 10^{14}$	1×10^{14}
244	3296	5.3×10^{15}	1.7×10^{15}
	3310	2.7×10^{15}	6×10^{14}
245	3296	1.02×10^{16}	1.2×10^{15}
	3310	6.6×10^{15}	6×10^{14}
246*	3296	$< 10^{14}$	5×10^{14}
	3310	$< 10^{14}$	7×10^{13}
247	3296	2.46×10^{16}	3.6×10^{15}
	3310	1.65×10^{16}	1.8×10^{15}
	3323	9.5×10^{15}	7×10^{14}
	3338	7.0×10^{15}	5×10^{13}
	3513	2.7×10^{15}	5×10^{13}
	3543	3.4×10^{15}	1.3×10^{15}
	3701	2.71×10^{16}	3.6×10^{15}

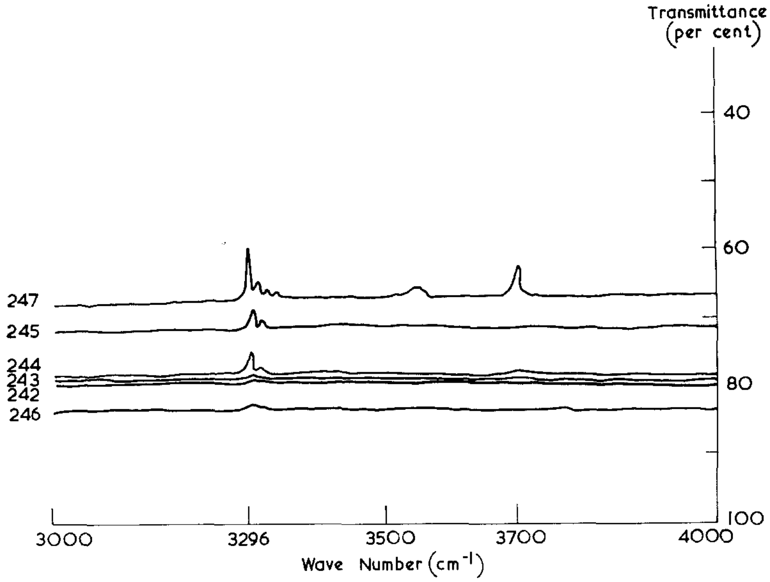

Figure 3 Infra-red spectra for the crystals of Fig. 2 after annealing in hydrogen.

Norton and one Spicer) known to produce cavities, from two Norton crystals known not to produce cavities, and from one Norton crystal of unknown behaviour, were chemically polished in hot orthophosphoric acid to give surfaces of similar high quality. Their thicknesses and infra-red absorption spectra were then measured, and the spectra are shown in Fig. 2. The three specimens from crystals known to produce cavities contained measurable amounts of hydroxyl complexes, and substitutional hydroxyl. The complexes gave rise to absorption peaks at 3296 and 3310 cm^{-1} in the two Norton specimens, and peaks at 3296, 3310, 3323, 3338, 3371, 3463, 3513, 3543 and 3701 cm^{-1} in the Spicer specimen. All these peaks were superimposed on broad substitutional OH bands. No hydroxyl complexes were detected in the two specimens from Norton crystals that were known not to produce cavities, nor in the crystal of unknown behaviour, but a broad, shallow, substitutional OH band was found in all three cases. Table III presents OH concentrations calculated from the spectra of Fig. 2.

All the specimens listed in Table III were annealed in hydrogen at 1230°C for 20 h, chemically polished to restore their surfaces to their original optical condition, and their absorption spectra were again measured. These spectra are shown in Fig. 3. All three specimens that were expected to produce cavities did so, and their OH concentrations were drastically reduced. None of the other crystals produced cavities, but in two of them OH complexes were then just detectable, and all the substitutional OH^- had disappeared. OH^- concentrations calculated from these spectra are also presented in Table III. It is considered that an absorption of 0.2% above background level is detectable. This corresponds to a concentration of 10^{14} OH^- per cm^3.

TABLE IV Comparison of OH^- ions lost with H atoms in cavities

Specimen number	Before H_2 anneal OH^- per cm^3	After H_2 anneal OH^- per cm^3	Change in OH^- per cm^3	Cavity volume (cm^3 per cm^3)	Number of H atoms in cavities	Ratio of H atoms to OH^- ions
244	8×10^{15}	2.3×10^{15}	5.7×10^{15}	5.4×10^{-6}	1.16×10^{17}	2.0
245	1.7×10^{16}	1.8×10^{15}	1.5×10^{16}	3.4×10^{-5}	7.29×10^{17}	4.9
247	9.0×10^{16}	1.1×10^{16}	7.9×10^{16}	2.4×10^{-4}	5.14×10^{18}	6.5

5. Correlation of the decrease in OH^- concentration with the appearance of hydrogen in cavities

In the three specimens in Table III that produced cavities, representative regions were photographed at a known magnification, and every cavity on the photographs was measured. Histograms of frequency of occurrence in each size range against size range were constructed, and from these the approximate total volume of cavities in the crystals was computed. Taking the average pressure of hydrogen in the cavities as 400 atm, the number of hydrogen atoms in the cavities in each specimen was calculated, assuming that the hydrogen was present as molecules. Table IV compares the amounts of hydroxyl disappearing and the amount of hydrogen appearing, and these quantities are not too dissimilar, considering the simplifying assumption made in the calculations of OH^- concentrations.

After the measurements for Table III had been made, the three specimens containing cavities were each cleaved to give three or four slices, and infra-red spectra obtained for the slices. Absorption coefficients for three hydroxyl peaks are plotted in Fig. 4, in which the extent of the cavity-containing zones is also shown. At the limits of these zones the average hydroxyl concentration was $\sim 1.5 \times 10^{15}$ ions cm^{-3}, which is, therefore, the minimum concentration required for cavity formation. The shapes of the hydroxyl distribution curves indicate that, in the regions where cavities did not form, hydroxyl complexes were lost to the crystal surfaces.

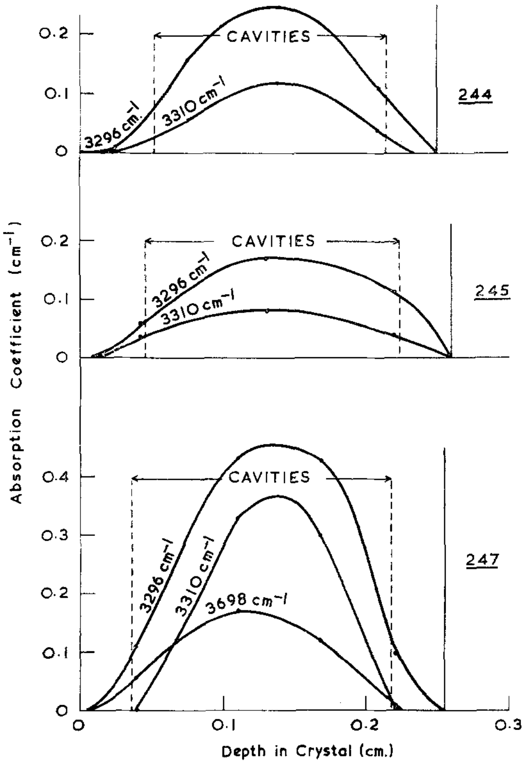

Figure 4 Hydroxyl distribution after annealing in hydrogen the three crystals of Figs. 2 and 3 that produced cavities. The extent of the cavities is marked by dashed vertical lines.

6. Hydroxyl distribution after annealing in argon

The effect of temperature alone on hydroxyl distribution was investigated by annealing in argon for 10 h at 1250°C a specimen from the same crystal as specimen 245. Infra-red spectra were taken before and after annealing, and also after cleaving the specimen into four slices. As shown in Table V, annealing in argon produced an 80% increase in the concentration of OH^- complexes. At the same time the absorption spectra showed a decrease in the concentration of substitutional OH^- ions. The distribution of the OH complexes after annealing is shown in Fig. 5, which shows that, particularly in the interior of the specimen, extra (OH-V) and OH-VI) complexes were formed. The source of OH^- for the new OH^- complexes was, therefore,

TABLE V OH^- content of crystals before and after annealing in argon

Treatment	Thickness (cm)	Peak wave number (cm^{-1})	Absorption coefficient (cm^{-1})	Band width (eV)	OH^- complex conc. (cm^{-3})
Before anneal	0.435	3296	0.240	9×10^{-4}	2.6×10^{15}
		3310	0.088	1.1×10^{-3}	1.2×10^{15}
After argon anneal	0.435	3296	0.360	1.2×10^{-3}	5.1×10^{15}
		3310	0.125	1.2×10^{-3}	1.8×10^{15}

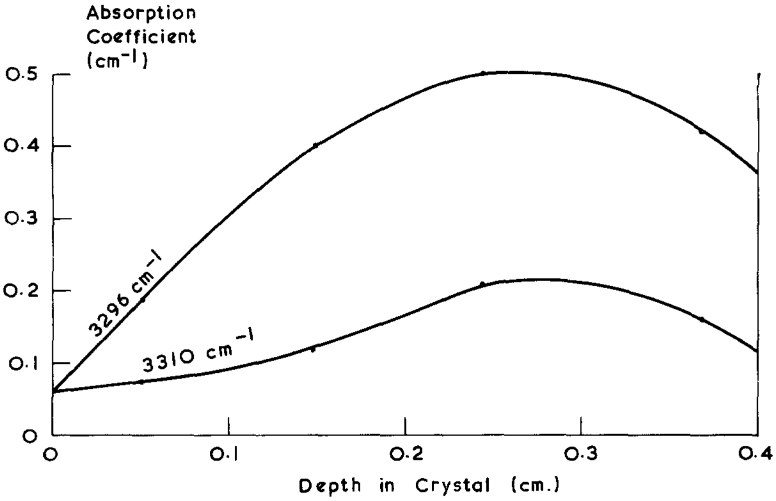

Figure 5 Hydroxyl distribution in a MgO crystal after annealing in argon.

the substitutional hydroxyl, and the vacancies required probably were supplied by the thermodynamic increase in vacancy concentration due to the temperature.

7. Cavity development

Careful study of hydrogen annealed crystals using optical and scanning electron microscopy after annealing times ranging from 20 min to 200 h revealed the following cavity development sequence:

(1) After 20 min at 1000° C no cavities could be seen, even using ultramicroscopy techniques. However, on cleaved crystals, the etching method described by Bowen and Clarke [4] revealed thin sheets of impurities on $\{100\}$ planes, with small dislocation arrays, decorated with impurities, around their perimeters, as shown in Fig. 6.

(2) Annealing for 40 min at 1000° C produced thin, square entities with sides parallel to $\langle 110 \rangle$, and rounded corners, which were visible both by ultramicroscopy and in reflected light, as shown in Fig. 7. At this stage it was possible, by quenching the crystals in water, to cause these entities to behave as cleavage cracks and expose themselves on cleaved surfaces. Scanning electron microscopy then showed that they consisted, of assemblies of many discrete micro-cavities often in rows as seen in Fig. 8.

(3) Longer annealing periods caused progressive coalescence of the micro-cavities to produce cruciform structures as shown in Figs. 9 and 10 and finally, after 20 to 200 h, lens-shaped cavities like the ones shown in Fig. 1 were produced. Each cavity was by this stage surrounded by extensive dislocation arrays which are revealed in Fig. 11 by etching a cleaved cross-section in sulphuric acid/ammonium

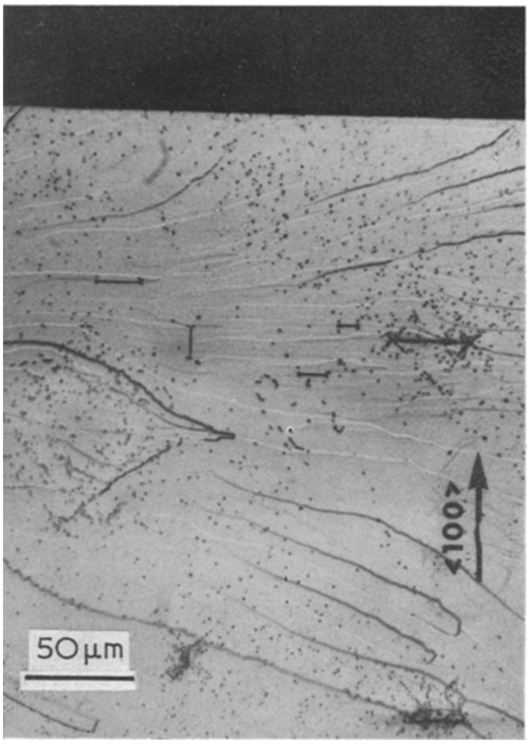

Figure 6 Embryo cavities at a very early stage in their formation, cleaved through and etched to reveal impurity concentrations.

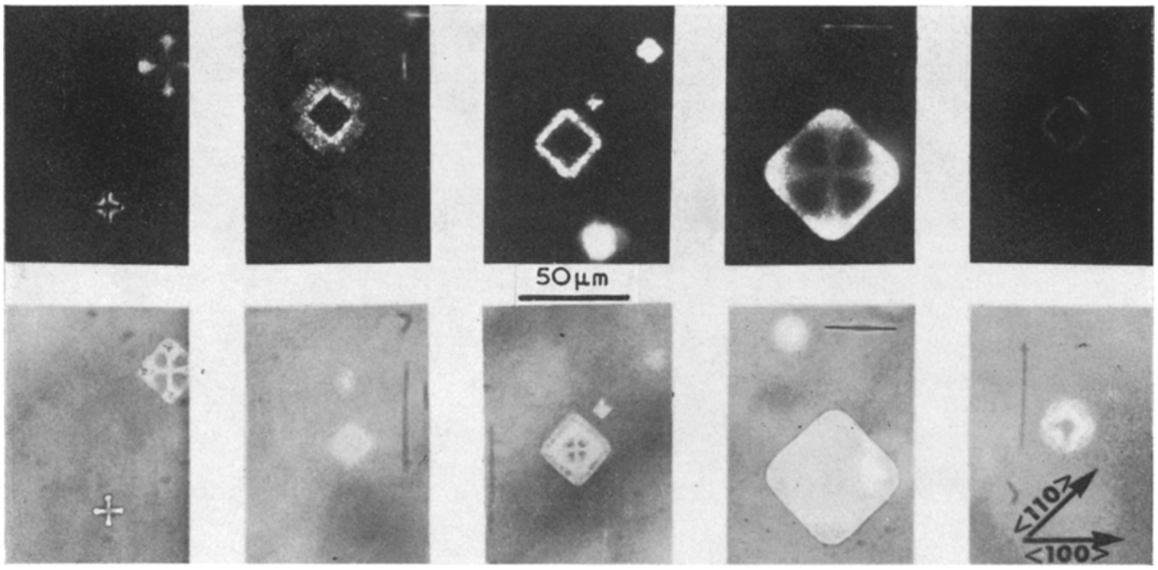

Figure 7 Cavities at early stages in their formation revealed by ultramicroscopy (upper row) and reflected light (lower row).

chloride solution [5]. The dislocation arrays imply the presence of stress fields around the cavities. Examination in transmitted, polarized light, as shown in Fig. 12, confirms their existence, which is due to the high pressure hydrogen. Measurement of the relative retardation around the cavity in Fig. 12 using Sénarmont compensation gave a maximum principal stress difference of 4.3×10^7 N m^{-2}, which agrees fairly closely with the mean hydrogen pressure derived from the gas release experiments.

8. A mechanism for the formation of hydrogen-filled cavities in crystals annealed in reducing atmospheres

It has been shown that cavities, produced by annealing MgO crystals in reducing gases, contained high pressure hydrogen, and that the source of the hydrogen was hydroxyl impurity within the crystals. Any mechanism for cavity formation must, therefore, explain the function of the reducing atmosphere, the conversion of hydroxyl to hydrogen, and the appearance of the latter under high pressure in the cavities. Since the presence of hydrogen in the cavities in both

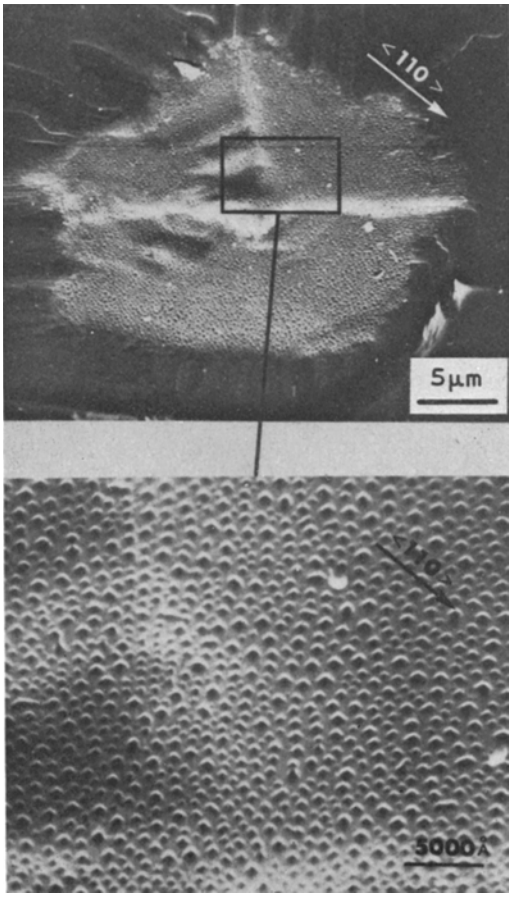

Figure 8 Scanning electron microscope photographs showing an early stage in the development of a lenticular cavity.

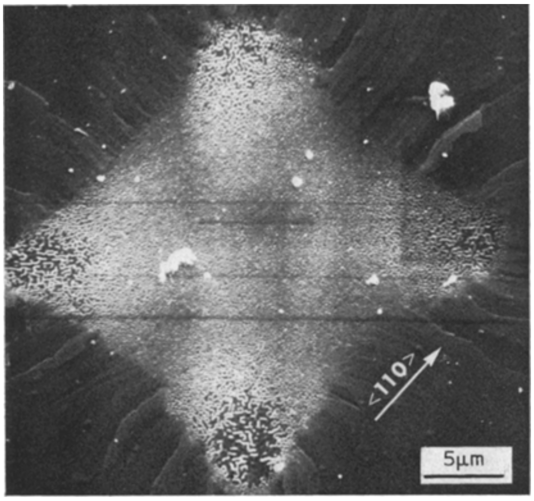

Figure 9 A scanning electron microscope photograph showing a later stage in the development of a cavity than the one in Fig. 8.

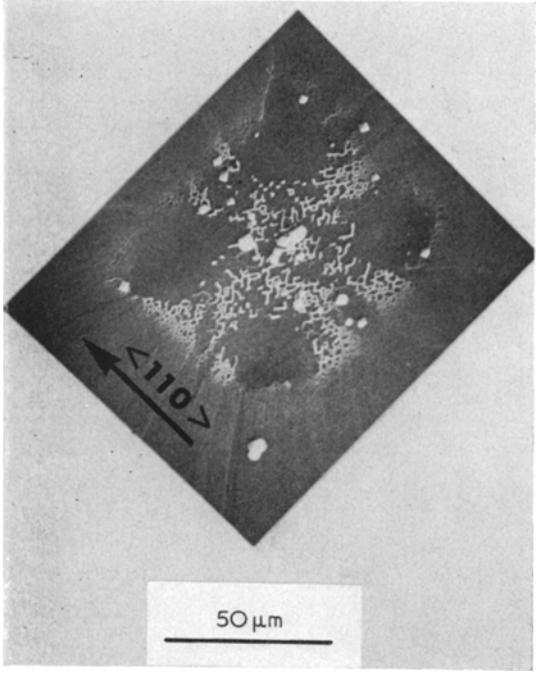

Figure 10 A scanning electron microscope photograph showing a still later stage in cavity development than that in Fig. 9.

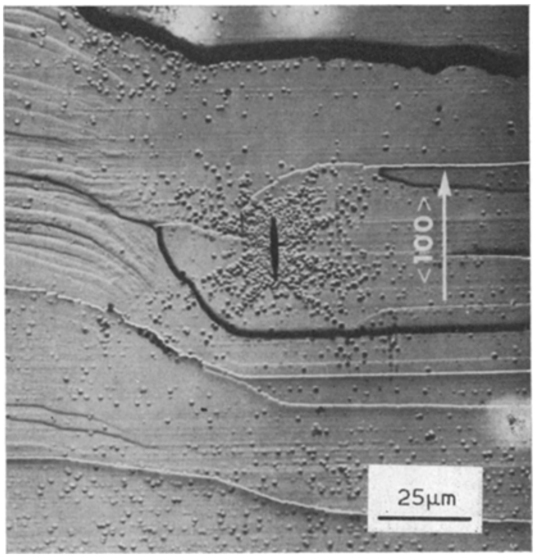

Figure 11 A cross-section of a lenticular cavity, exposed by cleavage, and etched to reveal dislocations.

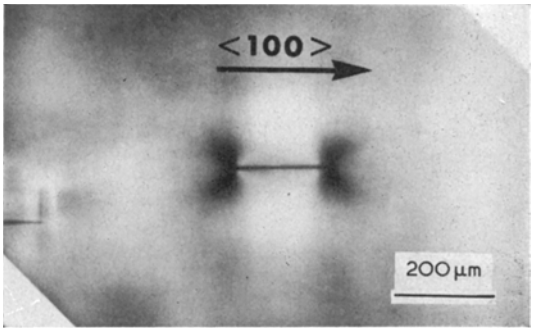

Figure 12 A transmitted, polarized light photograph, showing strain fields around a lenticular cavity.

slowly and rapidly cooled crystals indicates that the gas did not precipitate during cooling, the mechanism must also explain the accumulation of hydrogen in the cavities during their growth. Other factors to be considered are the hydroxyl and cavity distributions after hydrogen annealing and changes in the hydroxyl distribution during annealing. The following mechanism is postulated:

(1) The function of the reducing atmosphere is to remove oxygen ions from the surface of the MgO. Under thermodynamic equilibrium conditions the reaction

$$H_2 + MgO \rightarrow H_2O + Mg$$

would not be expected to occur, since ΔG is positive but, under the non-equilibrium conditions imposed by a flowing dry hydrogen atmosphere, the reaction might occur, and be encouraged by removal of the water produced. Removal of oxygen, as OH^-, from a crystal containing hydroxyl impurity, could more readily be accomplished by the reaction,

$$H + Mg - OH \rightarrow H_2O + Mg$$

and this reaction also would be favoured in the non-equilibrium conditions produced by a flowing atmosphere. This reaction could be maintained by migration of protons to the surface by the tunnelling mechanism of Freund and Gentsch [6]. An indication that one, or both, of the above reactions occurs is given by the fact that the water content of the furnace outlet gas increased during annealing experiments. Support for the second reaction is afforded by the hydroxyl concentration gradient results shown in Fig. 4.

The effect of carbon monoxide can be explained in a similar manner. The reaction,

$$CO + MgO \rightarrow CO_2 + Mg$$

has approximately the same ΔG as the above reaction between hydrogen and MgO, and might, therefore, also remove oxygen ions in non-equilibrium conditions.

(2) Removal of an oxygen ion or a hydroxyl ion from the surface creates either an oxygen vacancy plus two electrons or an oxygen vacancy plus one electron, as follows

$$H_2 + MgO \longrightarrow H_2O + Mg + \boxed{\text{O}} + 2e$$
$$H + Mg - OH \longrightarrow H_2O + Mg + \boxed{\text{O}} + e$$

$\boxed{\text{O}}$ is an oxygen vacancy carrying an effective double positive charge. e is an electron.

Wertz *et al.* [7] showed that the creation of oxygen vacancies and liberation of electrons in MgO could occur at 1200°C, even in vacuum, and they considered the trapping of the electrons by trivalent impurities.

(3) The oxygen vacancies and electrons diffuse into the crystal, possibly in association. The driving force for this is the concentration gradient set up by their creation at the surface.

(4) Within the crystal the oxygen vacancies and electrons encounter hydroxyl/magnesium vacancy complexes and the following reaction occurs.

$$\boxed{\text{Mg}} - OH^- + \boxed{\text{O}} + e \longrightarrow \boxed{\text{Mg}}\boxed{\text{O}} + H + O^{2-}$$

$\boxed{\text{Mg}}\boxed{\text{O}}$ is a divacancy

A divacancy containing a hydrogen atom is formed, which may diffuse and condense with similar entities to form a cavity nucleus containing hydrogen gas. Henderson *et al.* [2] showed by esr measurements that vacancy pairs formed in MgO by neutron irradiation could diffuse to cavities formed during a previous anneal in hydrogen. In the present case the divacancies and hydrogen atoms form "centres of hydrostatic vacancies". Such centres, according to Amelinckx *et al.* [8], should be capable of rapid diffusion, since this implies only the transfer of material from one side of the nucleus to the other. They will, therefore, diffuse until they are trapped, for example, at dislocations, where they can agglomerate to form cavities, or until they reach a surface. The appearance of pits on the surfaces of specimens annealed in reducing atmospheres shows that vacancies of both types arrive there, and the existence of cavity-free zones near the surfaces supports the idea that divacancies formed within these zones diffuse to the surface. A theoretical estimate of the hydrogen pressure in a cavity, if each magnesium vacancy contributed is accompanied by a hydrogen atom, and the atoms form hydrogen molecules, is 5×10^7 N m^{-2}. This figure is very close to the experimentally determined value, 4×10^7 N m^{-2}, and provides good support for the proposed mechanism.

9. Discussion

The mechanism described above has a close parallel in the work of Amelinckx *et al.* [8], in which hydrogen annealing of potassium chloride crystals containing nitrate impurity ions produced cavities containing oxygen and nitrogen. The reaction at the KCl surface deduced by Amelinckx *et al.* was,

$$H_2 + 2\,KCl \rightarrow 2\,HCl + 2\,K^+ + 2e + 2\square^-$$

where e is an electron, $\square^-$ is a chlorine vacancy. The parallel reaction in the present work, using the same notation, is,

$$H_2 + MgO \rightarrow H_2O + Mg^{2+} + 2e + \square^{2-}$$

where $\square^{2-}$ is an oxygen vacancy.

This parallel can be taken even further, in that, in both cases, the electrons and vacancies produced at the surface are involved in the formation of gas-filled cavities in the interior. In both cases, also, the appearance of gas-filled cavities accompanies the disappearance of anion impurities, which suggests that similar reactions are also involved at this stage. The reaction for the MgO case is given in Section 3, and the reaction proposed by the author for the KCl case is

$$2(\boxed{\mathrm{K}}-\mathrm{NO_3^-}) + 2\,\boxed{\mathrm{Cl}} + 2e \rightarrow 2\,\boxed{\mathrm{K}}\boxed{\mathrm{Cl}} + \mathrm{N_2} + 2\mathrm{O_2} + 2\mathrm{O^{2-}}.$$

In both the MgO and KCl cases, heterogeneous nucleation of cavities on dislocations decorated with impurity precipitates was observed.

Other studies with parallel results were those of Barr and Morrison [9] and Barr *et al.* [10], who produced cavities in sodium chloride crystals by heating them at 700°C in chlorine. They showed conclusively that the effect depended on the presence in the crystals of hydroxyl impurity. The cavities contained gas under pressure, but the gas was not analysed. However, by analogy with the present work, it is likely that the gas was hydrogen. Barr and Morrison [9] also observed cavity formation in a carbonate-doped KCl crystal annealed in chlorine. The cavities were filled with unidentified gas, at pressures greater than one atmosphere, which they presumed was CO_2. A possible reaction for producing the cavities and gas is

$$\boxed{\mathrm{K}}-\mathrm{CO_3^-} + \boxed{\mathrm{Cl}} + e \rightarrow \boxed{\mathrm{K}}\boxed{\mathrm{Cl}} + \mathrm{CO_2} + \mathrm{O^{2-}}.$$

A general principle is thus apparent in the results of Amelinckx *et al.* [8], Barr *et al.* [9, 10] and the present work, i.e. a special environment by reacting with a crystal surface, causes a second reaction within the crystal which converts an anion impurity into a permanent gas, and produces gas-filled cavities. Although the reactants and gaseous products may be quite different, the mechanisms involved are similar.

10. Conclusions

(1) The defects causing cloudiness in some MgO crystals annealed in reducing gases are thin, lenticular cavities, up to 200 μm diameter lying close to {100} planes.

(2) The cavities contain hydrogen gas under ~ 400 atm pressure.

(3) The cavities are produced only in crystals containing hydroxyl impurities in the form of hydroxyl/cation vacancy complexes (V_{OH} centres).

(4) The mechanism of formation of the gas-filled lenticular cavities involves the creation of oxygen vacancies and electrons at the surface by chemical reduction, and reaction of these in the interior of the crystal with V_{OH} centres to form divacancies containing hydrogen atoms. Agglomeration of divacancies produces micro-cavities containing hydrogen molecules, and the micro-cavities then coalesce to form lenticular cavities.

(5) The results of this work, coupled with the author's interpretation of those of other workers, allow the postulation of a general principle which may be applicable to many reducing gas/ionic crystal systems: a reducing gas, by reacting with the surface of an ionic crystal, may cause a second reaction within the crystal which converts an anion impurity into a permanent gas and produces gas-filled cavities.

Acknowledgements

The author wishes to thank Dr R. D. King for introducing him to infra-red analytical techniques and the associated calculations, Mr J. Dyson for the precision density measurements, Dr D. H. Bowen and Mr R. Steadman for valuable discussions during the work. Thanks are also due to Dr R. W. Davidge for comments on the manuscript and the UKAEA for supporting the work, which is based on a thesis submitted to the University of Bradford in partial fulfilment for the degree of Doctor of Philosophy.

References

1. A. BRIGGS, *J. Mater. Sci.* **10** (1975) 729.
2. B. HENDERSON, D. H. BOWEN, A. BRIGGS and R. D. KING, *J. Phys. C.: Solid Stat. Phys.* **4** (1971) 1496.
3. A. D. LE CLAIRE, *Phil. Mag.* **14** (1966) 1271.
4. D. H. BOWEN and F. J. P. CLARKE, *Phil. Mag.* **8** (1963) 1257.
5. T. K. GHOSH and F. J. P. CLARKE, *Brit. J. Appl. Phys.* **12** (1961) 44.
6. F. FREUND and H. GENTSCH, *Ber. Deutsch. Keram. Ges.* **44** (1967) 51.
7. J. E. WERTZ, P. AUZINS, J. H. E. GRIFFITHS and J. W. ORTON, *Disc. Faraday Soc.* **26** (1958) 66.
8. S. AMELINCKX, W. MAENHAUT-VAN DER VORST and W. DEKEYSER, *Acta Metallurgica* **7** (1959) 8.
9. L. W. BARR and J. A. MORRISON, *J. Appl. Phys.* **31** (1960) 617.
10. L. W. BARR, F. P. KOFFYBERG and J. A. MORRISON, *J. Appl. Phys.* **33** (1962) 225.

Received 11 November and accepted 25 November 1974.